

NJC

Accepted Manuscript



This is an *Accepted Manuscript*, which has been through the Royal Society of Chemistry peer review process and has been accepted for publication.

Accepted Manuscripts are published online shortly after acceptance, before technical editing, formatting and proof reading. Using this free service, authors can make their results available to the community, in citable form, before we publish the edited article. We will replace this *Accepted Manuscript* with the edited and formatted *Advance Article* as soon as it is available.

You can find more information about *Accepted Manuscripts* in the [Information for Authors](#).

Please note that technical editing may introduce minor changes to the text and/or graphics, which may alter content. The journal's standard [Terms & Conditions](#) and the [Ethical guidelines](#) still apply. In no event shall the Royal Society of Chemistry be held responsible for any errors or omissions in this *Accepted Manuscript* or any consequences arising from the use of any information it contains.



www.rsc.org/njc

NJC



ARTICLE

Efficient Visible-Light Photocatalytic Heterojunctions Coupled by Plasmonic Cu_{2-x}Se and Graphitic Carbon Nitride

Received 00th January 20xx,
Accepted 00th January 20xx

DOI: 10.1039/x0xx00000x

www.rsc.org/

Jing Han,^{ab} Hong Yan Zou,^{ab} Ze Xi Liu,^a Tong Yang,^b Ming Xuan Gao^b and Cheng Zhi Huang^{ab}

Photocatalytic semiconductors have attracted considerable attention due to applications in the degradation of organic pollutants. However, the low solar-light harvesting and high electron-hole recombination rate limits the efficiency of photocatalysts. The newly developed localized surface plasmon resonance (LSPR) can offer a new opportunity to overcome the limited efficiency to some extent. In this study, the heterojunctions (Cu_{2-x}Se/g-C₃N₄) incorporating plasmonic semiconductor Cu_{2-x}Se with graphitic carbon nitride (g-C₃N₄) are proposed as visible light photocatalysts. Their photocatalytic performance is tested and proven via the degradation of methyl blue (MB) in aqueous solution. When the mass percentage composition of Cu_{2-x}Se reached 60%, the as-prepared composite exhibited the highest photocatalytic activity, which was almost 6.1 and 2.8 times as high as that of individual Cu_{2-x}Se and g-C₃N₄, respectively. The remarkable photocatalytic efficiency of such Cu_{2-x}Se/g-C₃N₄ heterojunction under visible light illumination due to both plasmonic enhancement of the catalyst and synergetic effect of the co-catalyst is shown. This work can provide a new methodology to develop stable and high efficient heterojunctions photocatalysts.

Introduction

Photocatalysis has proved to be a green and potential technology to solve environmental issues such as air and water pollution.¹ Much efforts have been made to focus on semiconductor-based photo-catalysts and photocatalytic processes using titanium dioxide (TiO₂) since the pioneering work of Honda in 1972,² wherein TiO₂ can only absorb ultraviolet (UV) light gap because of its large band. In nature, visible-light energy (about 48% of the solar spectrum) within solar spectra is far more abundant than UV energy (about 4% of the solar spectrum). Therefore, it has stimulated researchers to develop novel materials to enhance the response to the more abundant visible light to NIR photons.

It has reported that the localized surface plasmon resonance (LSPR) in the semiconductor can enhance the absorption of solar light throughout the visible to near-infrared light range by concentrating the incident photon energy in plasmon oscillations, and it can usually amplify the electromagnetic field of the surface inducing carrier separation in the semiconductor.³ The cation-deficient copper chalcogenides nanocrystals, with the high density of holes in the valence band often, show exciting plasmonic photo-

properties over UV to NIR region.⁴ Cu_{2-x}Se nanocrystals, as a *p*-type semiconductor with electron-hole pair which can be excited on absorption of a photon with energy as low as 1.0-2.2 eV, can absorb the long wavelengths of solar light for the upward energy transition, and thus have promising potential for photocatalytic activity. Even though, the photocatalytic performance of Cu_{2-x}Se nanocrystals is limited by the high recombination rate of the photogenerated free carriers. The pollution degradation by the copper chalcogenides nanostructures must be in the presence of H₂O₂, which can cause the second pollution and the cost push.⁵ To minimize electron-hole recombination, Lee et al designed photocatalysts with heterojunctions because the band level differences and inner electrostatic field in the heterojunction could provide the driving force for the separation of photogenerated electrons and holes.⁶

Graphitic carbon nitride (g-C₃N₄), as a *n*-type semiconductor, is one of promising candidate photocatalysts due to its electron-rich properties, suitable bandgap and high chemical stability.⁷ However, the photocatalytic performance of g-C₃N₄ is far from satisfactory due to the large optical band gap (2.7 eV, corresponds to a utilization of solar energy at $\lambda < 460$ nm). Design of heterojunctions with other semiconductors can supply an opportunity to yield an elevated visible light response.⁸ This methodology could significantly expand light response range to visible light region and could effectively promote photogenerated charge separation and transfer. However, the design strategy is limited to band matching of the semiconductors, most of which are not easily synthesized under mild conditions.

Herein, we developed a simple solvent-thermal route to synthesize plasmonic Cu_{2-x}Se/g-C₃N₄ heterojunctions composites with enhanced absorption throughout the visible to near-infrared light range. The promising photocatalytic activity was screened via the photocatalytic degradation of an

^aKey Laboratory of Luminescence and Real-Time Analytical Chemistry (Southwest University), Ministry of Education, College of Pharmaceutical Science, Southwest University, Southwest University, Chongqing, 400715, P. R. China. E-mail: chengzhi@swu.edu.cn, Tel: (+86) 23 68254659, Fax: (+86) 23 68367257.

^bCollege of Chemistry and Chemical Engineering, Southwest University C, Chongqing 400716, China.

[†]Electronic Supplementary Information (ESI) available: experiment details and characterization of Cu_{2-x}Se/g-C₃N₄ heterojunction. See DOI: 10.1039/x0xx00000x

organic dye (MB) in an aqueous solution under visible light illumination. This strategy might provide a new methodology to develop stable and high efficient photocatalysts.

Experimental

Preparation of $g\text{-C}_3\text{N}_4$

The $g\text{-C}_3\text{N}_4$ was synthesized by directly heating melamine according to a reported procedure.⁹ In detail, melamine was heated at 600 °C for 2 h under air condition with a ramp rate of about 3 °C min^{-1} for both of the heating and cooling processes. The obtained yellow product was the $g\text{-C}_3\text{N}_4$ powder.

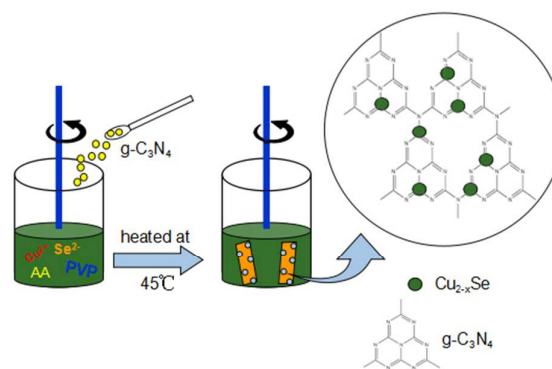
Preparation of $\text{Cu}_{2-x}\text{Se}/g\text{-C}_3\text{N}_4$

A certain amount of the as-prepared $g\text{-C}_3\text{N}_4$ was dispersed in 8 mL of deionized water and sonicated for 30 min. Then 0.2 mL 0.05 M SeO_2 and 0.4 mL 15 $\mu\text{g}/\text{mL}$ Vc was added, successively. After 10 min, a mixed solution of 0.4 mL 0.1M $\text{CuSO}_4\cdot 5\text{H}_2\text{O}$ and 0.8 mL 15 $\mu\text{g}/\text{mL}$ Vc were added under vigorous stirring at 30 °C for 0.5 h, then heated up to 45 °C. The resulting mixture was allowed to proceed under vigorous stirring at room temperature in 10 h until a green solution was obtained. The solution was centrifuged at 10000 rpm for 10 min and purified through a 10 kDa dialysis membrane for 24 hours with distilled water.

A series of $\text{Cu}_{2-x}\text{Se}/g\text{-C}_3\text{N}_4$ composites with different mass amounts of Cu_{2-x}Se were prepared marked as 20 wt%, 40 wt%, and 60 wt%. As a reference, the pure Cu_{2-x}Se was prepared without adding $g\text{-C}_3\text{N}_4$ under the same conditions. Moreover, a mechanically mixed sample (the mass ratio of $g\text{-C}_3\text{N}_4$ and Cu_{2-x}Se was 2:3) was obtained by grinding 4.8 mg of $g\text{-C}_3\text{N}_4$ with 7.2 mg of Cu_{2-x}Se .

Photocatalytic test

As a common organic pollutant, MB was employed to evaluate the photocatalytic activities of the as-prepared photocatalysts under visible-light ($\lambda > 420 \text{ nm}$) degradation illuminated by a 500W xenon lamp. 12 mg of the powder photocatalysts were dropped into quartz tubes which were containing 50 mL MB solution ($2 \times 10^{-5} \text{ mol L}^{-1}$), respectively. Then, the above solution was ultrasonic dispersion for 10 min and stirred for 30 min in dark to achieve an adsorption-desorption equilibrium between the photocatalyst powder and MB. Turn on the light and the photocatalytic reaction systems were exposed to visible light irradiation. At the same intervals, 0.5 mL of the mixture were taken out to centrifuge tubes, and the catalysts were removed out of the suspensions (10000 r/min, 5 min). The centrifuged solution was analysed by recording the maximum absorption band (664 nm) and UV-vis spectra were recorded by Hitachi U-3600.



Scheme 1. Schematic illustration of the formation process of $\text{Cu}_{2-x}\text{Se}/g\text{-C}_3\text{N}_4$ heterojunctions.

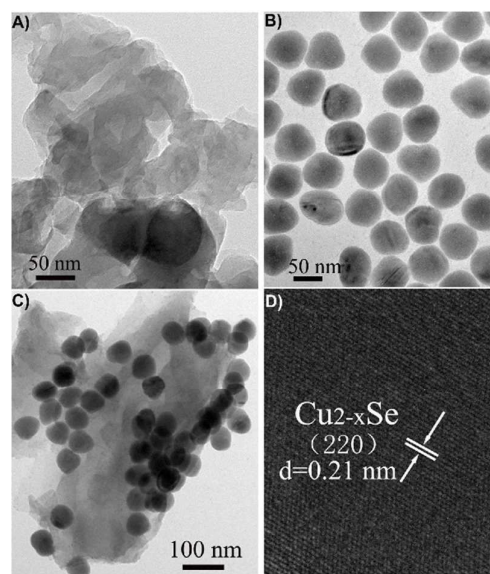


Fig. 1 Structure characterization of the photocatalysts. TEM images of $g\text{-C}_3\text{N}_4$ (A), Cu_{2-x}Se (B), 60 wt% $\text{Cu}_{2-x}\text{Se}/g\text{-C}_3\text{N}_4$ (C) and the HRTEM image of the Cu_{2-x}Se nanoparticle of the $\text{Cu}_{2-x}\text{Se}/g\text{-C}_3\text{N}_4$ heterojunctions (D).

Results and discussion

Structure and property analysis

The $\text{Cu}_{2-x}\text{Se}/g\text{-C}_3\text{N}_4$ heterojunction materials were fabricated by a simple solvent-thermal route as shown in Scheme 1. $\text{CuSO}_4\cdot 5\text{H}_2\text{O}$, SeO_2 and VC solutions were mixed with dispersed $g\text{-C}_3\text{N}_4$. With water-thermal reaction, small distributed uniform spherical Cu_{2-x}Se nanoparticles were successfully deposited on the surface of $g\text{-C}_3\text{N}_4$. Typical morphologies of the as-prepared heterojunctions (SEM, Fig.S1; TEM images, Fig. 1 and Fig. S2, ESI[†]) showed that the bulk $g\text{-C}_3\text{N}_4$ was quite rough, ranging from hundreds of nanometers to several micrometers (Fig. 1A). Small spherical Cu_{2-x}Se nanoparticles with 50 nm in diameter (Fig. 1B) were successfully deposited on the surface of $g\text{-C}_3\text{N}_4$ as nanoislands (Fig. 1C). Fringes with an inter-planar spacing of 0.21 nm were identified (Fig. 1D), which were attributed to the (220) diffraction plane of Cu_{2-x}Se nanoparticles.¹⁰ Elemental analysis was determined by SEM-EDS (Fig. S3, ESI[†]) showed an average Cu/Se atomic ratio of 1.69/1 with averaging among several particles. The Cu_{2-x}Se

nanoparticles were distributed separately on $g\text{-C}_3\text{N}_4$ as nanoislands, which could not only improve the dispersion property of layered materials but also offer more photocatalytic reaction sites, and the heterojunction structure was formed.

The XRD patterns of the $\text{Cu}_{2-x}\text{Se}/g\text{-C}_3\text{N}_4$ photocatalysts were measured (shown in Fig. 2). For $g\text{-C}_3\text{N}_4$, the strong peak located at 27.42° was ascribing to the (002) plane of the stacking of the conjugated aromatic system. The other peak at 12.74° as the (100) plane corresponded to the in-plane structural packing motif of trietazine units.¹¹ New peaks at 44.85° and 53.41° were observed for $\text{Cu}_{2-x}\text{Se}/g\text{-C}_3\text{N}_4$ which matched well with the (220) and (311) crystal planes of the standard XRD data for the cubic berzelianite phase of Cu_{2-x}Se (PDF card 06-0680),¹² and the intensity of peak at 53.41° increased as the increasing content of the Cu_{2-x}Se .

The FT-IR spectra of $\text{Cu}_{2-x}\text{Se}/g\text{-C}_3\text{N}_4$ heterojunctions were shown in Fig. 3. In the FT-IR spectrum of $g\text{-C}_3\text{N}_4$, the bands at 1648, 1562,

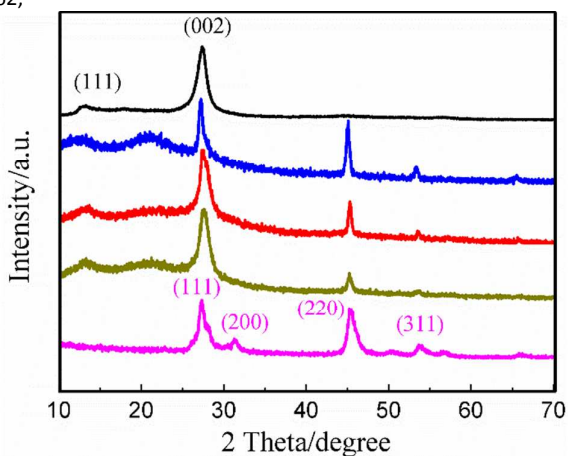


Fig. 2 XRD patterns of $g\text{-C}_3\text{N}_4$, Cu_{2-x}Se and $\text{Cu}_{2-x}\text{Se}/g\text{-C}_3\text{N}_4$ samples.

1456, and 1402 cm^{-1} should be assigned to typical stretching vibration modes of the heptazine-derived repeating units, while the

intense band at 804 cm^{-1} represented the out-of-plane bending vibration characteristic of heptazine rings,¹³ and the bands at 1237 cm^{-1} corresponded to stretching vibration of connected units of $\text{C-N}(\text{-C})\text{-C}$ or C-NH-C .¹⁴ For $\text{Cu}_{2-x}\text{Se}/g\text{-C}_3\text{N}_4$, the broad band at $3000\text{--}3700\text{ cm}^{-1}$ belonged to the N-H vibration due to partial condensation of the capping agent and the adsorbed water molecules,^{8d} and the band (652 cm^{-1}) corresponded to the vibration of -Se for Cu_{2-x}Se .¹⁵ All the characteristic peaks of $g\text{-C}_3\text{N}_4$ and Cu_{2-x}Se

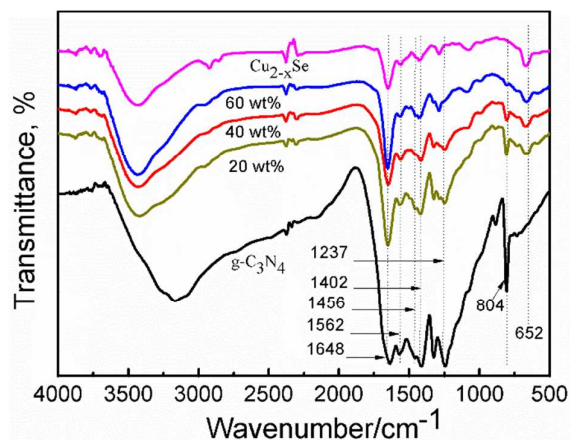


Fig. 3 FT-IR spectra of $g\text{-C}_3\text{N}_4$, Cu_{2-x}Se and $\text{Cu}_{2-x}\text{Se}/g\text{-C}_3\text{N}_4$ samples.

were observed in the $\text{Cu}_{2-x}\text{Se}/g\text{-C}_3\text{N}_4$ heterojunctions composition

The chemical compositions of the as-prepared heterojunctions were further characterized by XPS spectra (Fig. 4). As for $\text{Cu}_{2-x}\text{Se}/g\text{-C}_3\text{N}_4$, new Cu and Se peaks were observed, confirming the decoration of Cu_{2-x}Se nanoparticles on the $g\text{-C}_3\text{N}_4$ surface (Fig. 4A, B). The evolution of the Cu 2p XPS spectra contained in Fig. 4C showed a clear indication of monovalent copper. The peaks of 932.4 and 952.8 eV were ascribed to Cu 2p $3/2$ and Cu 2p $1/2$ which was mainly in the form of Cu (I). In addition, the Cu2p peak had a satellite line at 940–945 eV, which resulted from a little Cu (II) (Fig. 4C).^{10, 16} Since XPS is



NJC

ARTICLE

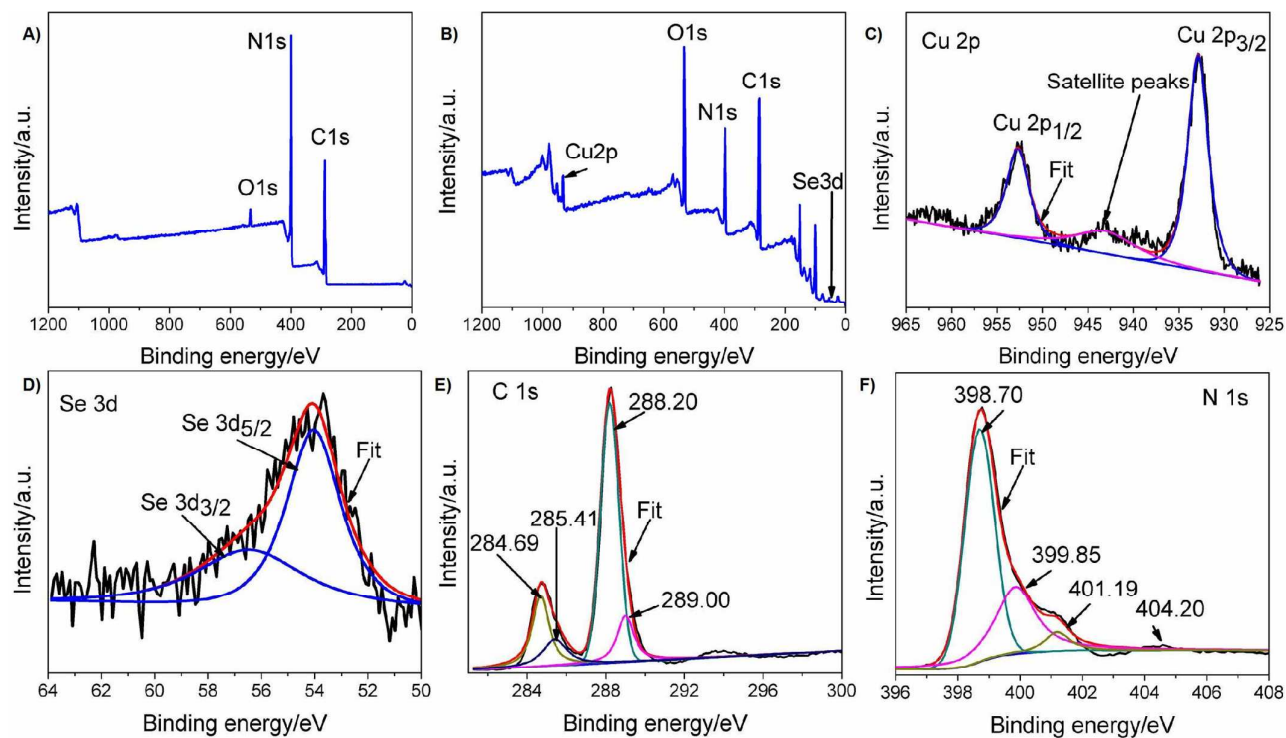


Fig. 4 (A) XPS spectra of the Cu_{2-x}Se (B) XPS spectra of the $\text{Cu}_{2-x}\text{Se}/\text{g-C}_3\text{N}_4$ heterojunctions. (C) XPS spectra of $\text{Cu } 2p_{1/2}$ and $\text{Cu } 2p_{3/2}$. (D) XPS spectra of $\text{Se } 3d$. (E) XPS spectra of $\text{C } 1s$, and (F) XPS spectra of $\text{N } 1s$.

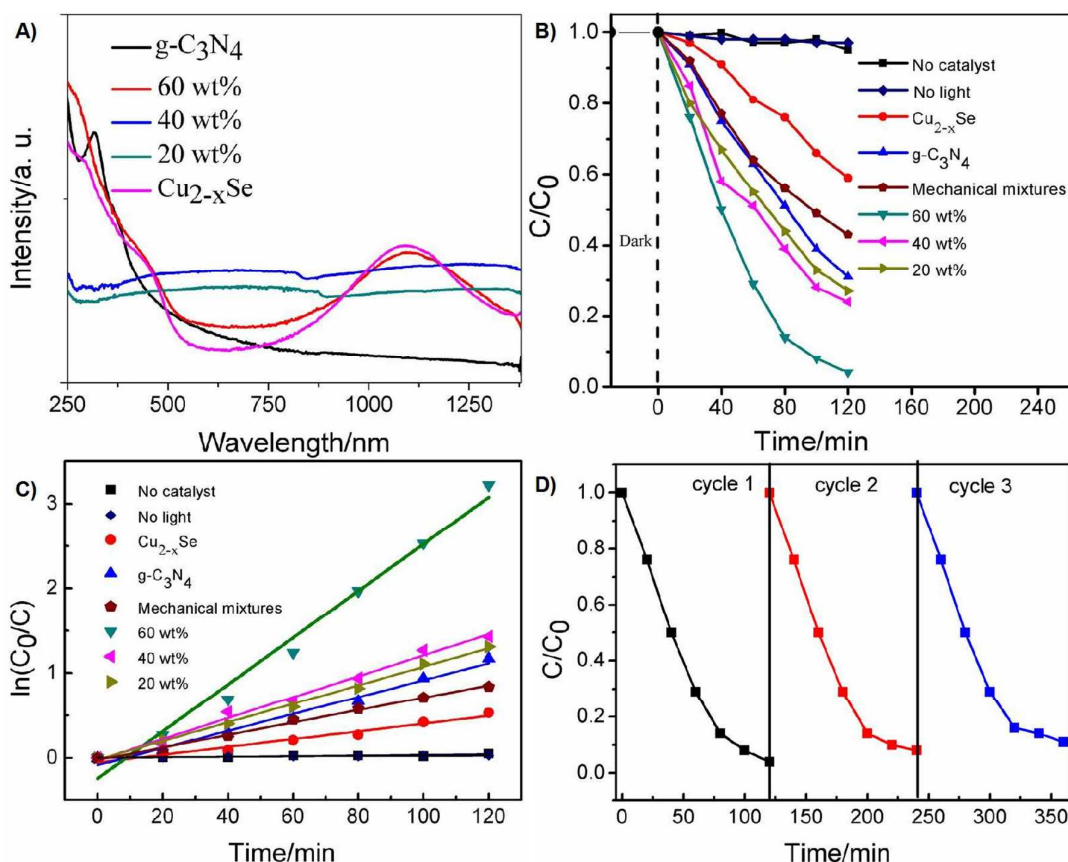


Fig.5 Photocatalytic activity of catalysts estimated by the degradation of MB under visible light irradiation (A) UV-vis-NIR spectra of the photocatalysts. (B) Photocatalytic degradation of MB in aqueous solution under different conditions. (C) $\ln(C_0/C)$ versus irradiation time for degradation of MB under different conditions. (D) Recyclability of the Cu_{2-x}Se/g-C₃N₄ heterojunctions in three successive experiments for the degradation of MB under visible-light irradiation.

primarily a surface characterization technique, the non-stoichiometric Cu_{2-x}Se in the 60 wt % Cu_{2-x}Se/g-C₃N₄ heterojunctions had the atom percentage of surface Cu(I) and Cu(II) as 4.86:1.¹⁷ The asymmetric peak at 54.2 eV contains Se3d 5/2 and Se3d 3/2 peaks was representative of the Se3d binding energy for lattice Se²⁻ (Fig. 4D).¹⁷

The C 1s spectra can be deconvoluted (in Fig. 4E). The major C peak at 288.20 eV was identified as sp²-bonded carbon (N-C=N), and the weaker one at 284.69 eV corresponded to graphitic carbon which was usually observed on the XPS characterization for carbon nitrides.¹⁸ The N 1s spectrum (Fig. 4F) could be fitted into three binding energies. Signals at 398.7 eV showed occurrence of C-N-C groups and 399.85 eV was related to either N-(C)₃ groups or amino groups ((C)₂-N-H). The 401.2 eV peak was weak and corresponded to N of N-(C)₃ in the aromatic cycles and 404.20 eV peak was attributed to the π-excitations.^{8c, 19}

The as-prepared Cu_{2-x}Se/g-C₃N₄ heterojunctions have enhanced absorption throughout the visible to NIR light range (Fig. 5A). Cu_{2-x}Se had the LSPR property at the NIR range, while the g-C₃N₄ shows the optical absorption threshold at ca. 460 nm. It was the LSPR property¹⁰ and the optical absorption threshold⁴ that made the Cu_{2-x}Se/g-C₃N₄ composites showed a broad and strong

absorption in the visible light region and even extended to near-infrared region. This result indicated that Cu_{2-x}Se/g-C₃N₄ could absorb photons with different energies owing to the interaction between Cu_{2-x}Se and g-C₃N₄, which were beneficial to the sunlight photocatalytic process.

In order to estimate the photocatalytic effect of the as-prepared Cu_{2-x}Se/g-C₃N₄ heterojunctions, methylene blue (MB), a common organic pollutant, was selected under visible-light irradiation ($\lambda > 420$ nm) (Fig. S5-S12, ESI[†]). As shown in Fig. 5B, there was almost no decreasing concentration of MB during the adsorption-desorption process due to the low surface area of the photocatalysts (Table S1) and the surface areas do not play a significant role in enhancing the photocatalytic activity of the Cu_{2-x}Se/g-C₃N₄. Fig. 5C revealed that the relationship between $\ln(C_0/C)$ and irradiation time was linear, indicating that the photocatalytic degradation of MB followed the pseudo-first-order kinetics.

$$\ln(C_0/C) = kt \quad (1)$$

Where C_0 and C were the equilibrium concentration of adsorption and the concentration of MB at the exposure time, t , respectively, and k was the apparent rate constant. The Cu_{2-x}Se/g-C₃N₄ heterojunctions composite with 60% mass ratios of Cu_{2-x}Se (60 wt % Cu_{2-x}Se/g-C₃N₄) exhibited the highest photocatalytic rate

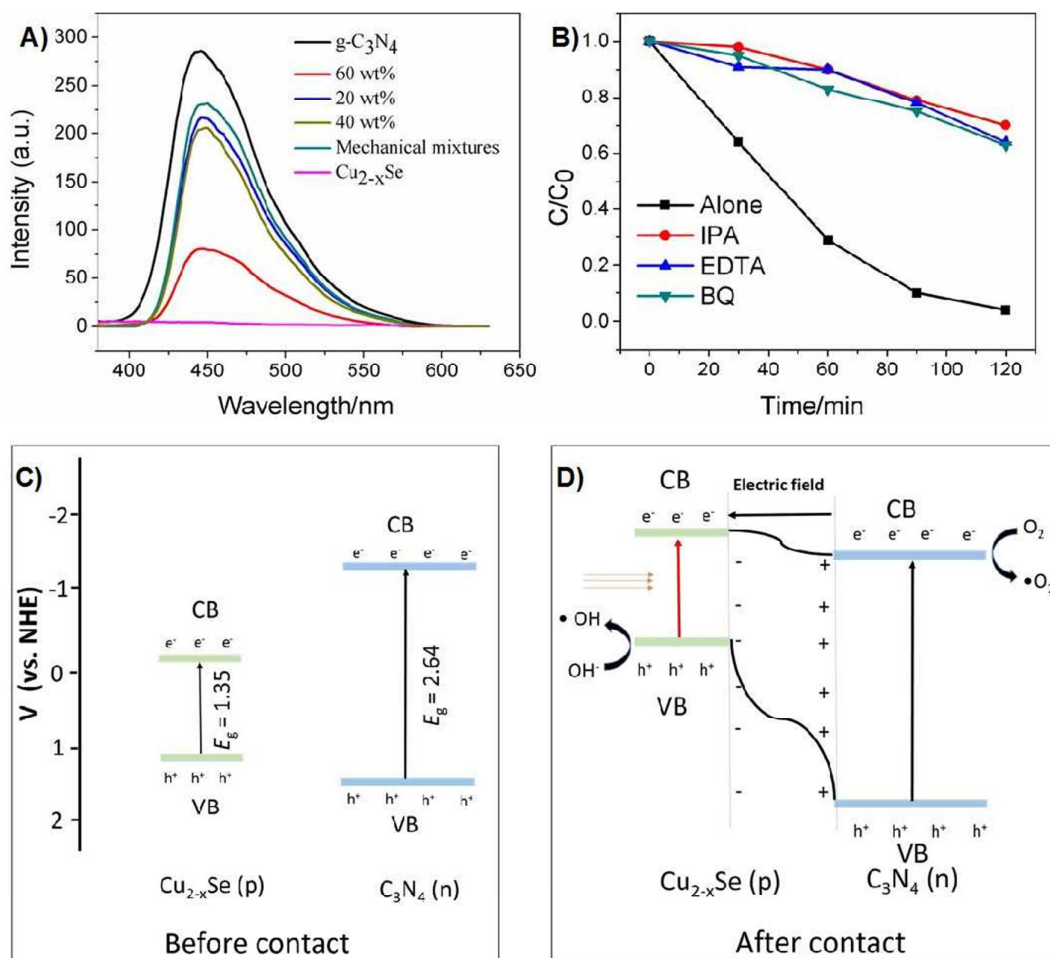


Fig. 6 Investigation of the photocatalytic mechanism. (A) The fluorescence spectra of the $g\text{-C}_3\text{N}_4$, Cu_{2-x}Se , $\text{Cu}_{2-x}\text{Se}/g\text{-C}_3\text{N}_4$ samples (with the mass of $g\text{-C}_3\text{N}_4$ as 12 mg in 50 mL 2 mM NaOH solution) and mechanical mixtures of 18 mg Cu_{2-x}Se and 12 mg $g\text{-C}_3\text{N}_4$ in 50 mL 2 mM NaOH solution (equal to the 60 wt% Cu_{2-x}Se). (B) Photocatalytic degradation of MB over $\text{Cu}_{2-x}\text{Se}/g\text{-C}_3\text{N}_4$ heterojunctions alone and with the addition of IPA, EDTA, and BQ. (C) The energy band structure diagram of Cu_{2-x}Se and $g\text{-C}_3\text{N}_4$ before heterojunction. (D) The energy band structure diagram of $\text{Cu}_{2-x}\text{Se}/g\text{-C}_3\text{N}_4$ heterojunctions

constant (k), which was almost 6.1 and 2.8 times as high as that of individual Cu_{2-x}Se and $g\text{-C}_3\text{N}_4$, respectively (Table S1). The $\text{Cu}_{2-x}\text{Se}/g\text{-C}_3\text{N}_4$ photocatalyst can be recycled several times (Fig. 5D) and was also very stable (Fig. S13, 14).

Fluorescence measurements, which were usually employed to investigate the migration, transfer and recombination processes of photogenerated electron-hole pairs in semiconductors.²⁰ A lower PL intensity is a general indication of a lower recombination of electron-hole pairs, resulting in higher photocatalytic activity.²¹ The bare $g\text{-C}_3\text{N}_4$ had a strong emission peak at 440 nm (Fig. 6A), which decreased remarkably in $\text{Cu}_{2-x}\text{Se}/g\text{-C}_3\text{N}_4$ composites with the increase mass ratio of Cu_{2-x}Se . Meanwhile, the FL of the mechanical mixtures of the same mass content of $g\text{-C}_3\text{N}_4$ with 60 wt% Cu_{2-x}Se were measured. It showed relatively weaker emission peak than $g\text{-C}_3\text{N}_4$ but stronger emission peak than all the $\text{Cu}_{2-x}\text{Se}/g\text{-C}_3\text{N}_4$ heterojunctions measured. While, the characteristic emission peak of $\text{Cu}_{2-x}\text{Se}/g\text{-C}_3\text{N}_4$ (60 wt%) was the most weak, indicating that the recombination of electron-hole pairs in $\text{Cu}_{2-x}\text{Se}/g\text{-C}_3\text{N}_4$ was hindered most greatly.

The photocatalytic activity of the photocatalyst always contributed to the active species such as photogenerated holes, $\bullet\text{OH}$ radicals, and $\bullet\text{O}_2^-$ in the photocatalytic process.⁸ Therefore, in order to examine the role of these reactive species, a series of radicals trapping experiments using isopropyl alcohol (IPA, 2 mM),²² ethylenediaminetetraacetate (EDTA, 2 mM),²³ and p-benzoquinone (BQ, 0.5 mM),²⁴ which are known as effective $\bullet\text{OH}$, holes, and $\bullet\text{O}_2^-$ scavengers for photocatalytic reaction, respectively, were applied to investigate the species involved in the process of photocatalytic degradation. Fig. 6B showed that holes, $\bullet\text{OH}$ radicals and $\bullet\text{O}_2^-$ indeed functioned during the catalytic process. In such case, a reasonable photocatalytic mechanism could be proposed.

Based on the results above, a possible photocatalytic mechanism of $\text{Cu}_{2-x}\text{Se}/g\text{-C}_3\text{N}_4$ heterojunctions under visible light irradiation was proposed and illustrated in Fig. C, D. The potentials of VB and CB of a semiconductor material can be estimated according to the following empirical equations,²⁵

$$E_{\text{VB}} = \chi - E^{\text{e}} + 0.5E_{\text{g}} \quad (2)$$

$$E_{CB} = E_{VB} - E_g \quad (3)$$

Wherein E_{VB} is the valence band edge potential, χ is the electronegativity of the semiconductor, which is the geometric mean of the constituent atoms, E^e is the energy of free electrons on the hydrogen scale (about 4.5 eV vs NHE). The χ values for $Cu_{2-x}Se$ and $g-C_3N_4$ were 4.96 and 4.64 eV, respectively. The band gap energy of $Cu_{2-x}Se$ and $g-C_3N_4$ in our experiment was 1.35 eV and 2.64 eV (Fig. S4, inset and see details in ESI[†]) of The E_{VB} of $Cu_{2-x}Se$ and $g-C_3N_4$ were calculated to be 1.14 and 1.46 eV, respectively. The E_{CB} of $Cu_{2-x}Se$ and $g-C_3N_4$ were estimated to be -0.21 and -1.18 eV, respectively. It is well known that the photocatalytic activities of photocatalysts, to a great extent, depend on the separation and transport of photogenerated charge carriers. When the $p-Cu_{2-x}Se$ and $n-C_3N_4$ were combined to form the $p-n$ heterojunction, an interfacial electric field could be built in the interface between $p-Cu_{2-x}Se$ and $n-C_3N_4$.²⁶ That fact caused an efficient separation of photogenerated electrons and holes to enhance the photocatalytic activity. Furthermore, because of the more positive potential of Cu^{2+}/Cu^{1+} (0.153 V), the photogenerated electrons on the CB of $Cu_{2-x}Se$ may in situ reduce Cu^{2+} to metallic Cu^{1+} , which also migrated the electron to inhibit the recombination of the photoexcited pairs. In such case, the photogenerated electrons on the CB of the $g-C_3N_4$ and $Cu_{2-x}Se$ can reduce the oxygen to generate active species $\bullet O_2^-$ ($O_2/\bullet O_2^-$, -0.046 V vs SHE) due to their more negative potential, which can further oxidize MB. Subsequently, it would combine with H^+ to produce H_2O_2 , finally decomposing into hydroxyl radicals $\bullet OH$ radicals.²⁷ These $\bullet OH$ radicals also played an additional role for the MB degradation. The holes in the VB of $g-C_3N_4$ diffused to the surface of catalyst particles and transferred to VB of $Cu_{2-x}Se$ to accomplish the separation of electron-hole pairs, which would be readily scavenged by H_2O or OH^- , leading to $\bullet OH$ radicals, and accelerated the MB degradation. These results matched well with the trapping experiments showing that the all the holes, $\bullet OH$ radicals and $\bullet O_2^-$ were involved in the process of the photocatalytic reaction.

Conclusions

In summary, efficient $Cu_{2-x}Se/g-C_3N_4$ plasmonic photocatalysts were successfully synthesized by a simple solvent-thermal method. The $Cu_{2-x}Se$ nanoparticles were dispersedly decorated on the surface of bulk $g-C_3N_4$. This novel heterojunctions were demonstrated to promote transfer and separation of photogenerated charge carriers driven by the band offsets, resulting in a significant enhancement in the photocatalytic activity for MB degradation under visible light irradiation. Furthermore, all the holes, $\bullet OH$ radicals and $\bullet O_2^-$ were the active species in the degradation process. This study might provide a new perspective for the design of high-performance photocatalysis by plasmonic semiconductor heterojunctioned with $g-C_3N_4$. And the nanostructure $Cu_{2-x}Se/g-C_3N_4$ heterojunctions can also be envisaged for further sustainable energy applications.

Acknowledgements

This study was financially supported by the National Natural Science Foundation of China (NSFC, Grant No.21375109) and Chongqing Postdoctoral Science Foundation funded project (Xm2014021).

Notes and references

§ Jing Han and Hong Yan Zou contributed to this work equally.

- a) M. R. Hoffmann, S. T. Martin, W. Choi and D. W. Bahnemann, *Chem. Rev.*, 1995, **95**, 69; b) M. D. Hernández-Alonso, F. Fresno, S. Suárez and J. M. Coronado, *Energy Environ. Sci.*, 2009, **2**, 1231; c) L. Q. Ye, J. Y. Liu, Z. Jiang, T. Y. Peng and L. Zan, *Appl. Catal., B* 2013, **142**, 1.
- A. Fujishima and K. Honda, *Nature*, 1972, **238**, 37.
- a) H. Zhang, X. Fan, X. Quan, S. Chen and H. Yu, *Environ. Sci. Technol.* 2011, **45**, 5731; b) W. Wang, H. Du, R. Wang, T. Wen and A. Xu, *Nanoscale* 2013, **5**, 3315; c) S. K. Cushing, J. T. Li, F. K. Meng, T. R. Senty, S. Suri, M. J. Zhi, M. Li, A. D. Bristow and N. Q. Wu, *J. Am. Chem. Soc.*, 2012, **134**, 15033; d) Z. W. Liu, W. B. Hou, P. Pavaskar, M. Aykol and S. B. Cronin, *Nano Lett.* 2011, **11**, 1111.
- a) F. Scotognella, G. Della Valle, A. R. Srimath Kandada, D. Dorfs, M. Zavelani-Rossi, M. Conforti, K. Miszta, A. Comin, K. Korobchevskaya, G. Lanzani, L. Manna and F. Tassone, *Nano Lett.*, 2011, **11**, 4711.; b) Y. Zhao, H. Pan, Y. Lou, X. Qiu, J. Zhu and C. Burda, *J. Am. Chem. Soc.*, 2009, **131**, 4253; c) A. Comin and L. Manna, *Chem. Soc. Rev.*, 2014, **43**, 3957; d) X. Liu, C. Lee, W. C. Law, D. Zhu, M. Liu, M. Jeon, J. Kim, P. N. Prasad, C. Kim and M. T. Swihart, *Nano Lett.*, 2013, **13**, 4333; e) X. Liu, X. Wang, B. Zhou, W. C. Law, A. N. Cartwright and M. T. Swihart, *Adv. Funct. Mater.*, 2013, **23**, 1256; f) S. Q. Lie, H. Y. Zou, Y. Chang, and C. Z. Huang, *RSC Adv.*, 2014, **4**, 55094; g) W. L. Li, S. Q. Lie, Y. Chang, X. Y. Wan, T. T. Wang, J. Wang, and C. Z. Huang, *J. Mater. Chem. B*, 2014, **2**, 7027.
- a) J. Kundu and D. Pradhan, *ACS Appl. Mater. Interfaces*, 2014, **6**, 1823; b) Q. W. Shu, L. Jing, M. X. Gao, J. Wang and C. Z. Huang, *CrystEngComm.*, 2015, **17**, 1374.
- a) H. G. Kim, P. H. Borse, W. Y. Choi and J. S. Lee, *Angew. Chem., Int. Ed.*, 2005, **44**, 4585; b) H. G. Kim, P. H. Borse, J. S. Jang, E. D. Jeong, O. S. Jung, Y. J. Suh and J. S. Lee, *Chem. Commun.*, 2009, 5889; c) A. Kudo and Y. Miseki, *Chem. Soc. Rev.*, 2009, **38**, 253; d) G. Wang, B. B. Huang, L. Wang, Z. Y. Wang, Z. Z. Lou, X. Y. Qin, X. Y. Zhang and Y. Dai, *Chem. Commun.*, 2014, **50**, 3814; e) R. Marschall, *Adv. Mater.*, 2014, **24**, 2421.
- a) X. Wang, K. Maeda, A. Thomas, K. Takanabe, G. Xin, J. M. Carlsson, K. Domen and M. Antonietti, *Nat. Mater.*, 2008, **8**, 76; b) Y. Zhao, F. Zhao, X. P. Wang, C. Y. Xu, Z. P. Zhang, G. Q. Shi and L. T. Qu, *Angew. Chem. Int. Ed.*, 2014, **53**, 13934; c) Y. Zheng, L. H. Lin, X. J. Ye, F. S. Guo and X. C. Wang, *Angew. Chem. Int. Ed.*, 2014, **53**, 11926; d) S. Kumar, S. Tonda, B. Kumar, A. Baruah and V. Shanker, *J. Phys. Chem. C*, 2013, **117**, 26135; e) J. Liu, Y. Liu, N. Y. Liu, Y. Z. Han, X. Zhang, H. Huang, Y. Lifshitz, S. T. Li, J. Zhong and Z. H. Kang, *Science*, 2015, **347**, 970.
- a) S. W. Cao and J. G. Yu, *J. Phys. Chem. Lett.*, 2014, **5**, 2101; b) H. Xu, J. Yan, Y. Xu, Y. Song, H. Li, J. Xia, C. Huang and H. Wan, *Appl. Catal., B*, 2013, **129**, 182; c) Y. F. Li, L. Fang, R. Jin, Y. Yang, X. Fang, Y. Xing and S. Y. Song, *Nanoscale*, 2015, **7**, 758; d) S. W. Zhang, J. X. Li, M. Y. Zeng, G. X. Zhao, J. Z. Xu, W. P. Hu and X. K. Wang, *ACS Appl. Mater. Interfaces*, 2013, **5**, 12735; e) Y. Feng, J. C. Shen, Q. F. Cai, H. Yang and Q. H. Shen, *New J. Chem.*, 2015, **39**, 1132; f) I. Aslam, C. Cao, M. Tanveer, W. S. Khan, M. Thair, M. Abid, F. Idrees, F. K. Butt, Z. Ali and N. Mahmood, *New J. Chem.*, 2014, **38**, 5462.
- X. D. Zhang, X. Xie, H. Wang, J. J. Zhang, B. C. Pan and Y. Xie, *J. Am. Chem. Soc.*, 2013, **135**, 18.
- a) D. Dorfs, T. Härting, K. Miszta, N. C. Bigall, M. R. Kim, A. Genovese, A. Falqui, M. Povia and L. Manna, *J. Am. Chem. Soc.*, 2011, **133**, 11175; b) S. Q. Lie, D. M. Wang, M. X. Gao and C. Z. Huang, *Nanoscale*, 2014, **6**, 10289.

Journal Name ARTICLE

- 11 Y. L. Tian, B. B. Chang, J. L. Lu, J. Fu, F. N. Xi and X. P. Dong, *ACS Appl. Mater. Interfaces*, 2013, **5**, 7079.
- 12 Z. T. Deng, M. Mansuripur and A. J. Muscat, *J. Mater. Chem.*, 2009, **19**, 6201.
- 13 S. C. Yan, Z. S. Li and Z. G. Zou, *Langmuir* 2009, **25**, 10397.
- 14 P. Niu, L. Zhang, G. Liu and H. Cheng, *Adv. Funct. Mater.*, 2012, **22**, 4763.
- 15 A. Beran, G. Giester and E. Libowitzky, *Miner. Petrol.*, 1997, **61**, 223.
- 16 I. Kriegel, C. Y. Jiang, J. Rodriguez-Fernandez, R. D. Schaller, D. V. Talapin, E. da Como and J. Feldmann, *J. Am. Chem. Soc.*, 2012, **134**, 1583.
- 17 S. C. Riha, D. C. Johnson and A. L. Prieto, *J. Am. Chem. Soc.*, 2011, **133**, 1383.
- 18 J. A. Singh, S. H. Overbury, N. J. Dudney, M. J. Li and G. M. Veith, *ACS Catal.*, 2012, **2**, 1138.
- 19 T. Y. Ma, Y. Tang, S. Dai and S. Z. Qiao, *Small*, 2014, **10**, 2382.
- 20 J. R. Lakowicz, *Principles of Fluorescence Spectroscopy*, 3rd ed., Springer: New York, 2006.
- 21 a) Y. F. Chen, W. X. Huang, D. L. He, Y. Situ and H. Huang, *ACS Appl. Mater. Interfaces*, 2014, **6**, 14405; b) J. S. Xu, T. J. K. Brenner, Z. P. Chen, D. Neher, M. Antonietti and M. Shalom, *ACS Appl. Mater. Interfaces*, 2014, **6**, 16481.
- 22 L. Jin, G. Zhu, M. Hojamberdiev, X. Luo, C. Tan, J. Peng, X. Wei, J. Li and P. Liu, *Ind. Eng. Chem. Res.*, 2014, **53**, 13718.
- 23 M. S. Elovitz and U. V. Gunten, *Ozone, Sci. Eng.*, 1999, **21**, 239.
- 24 Y. Zhang, N. Zhang, Z. Tang and Y. Xu, *Chem. Sci.*, 2013, **4**, 1820.
- 25 a) X. Lin, X. Y. Guo, W. L. Shi, L. N. Zhao, Y. S. Yan and Q. W. Wang, *J. Alloys Compd.*, 2015, **635**, 256; b) X. Lin, X. Y. Guo, W. L. Shi, L. N. Zhao, Y. S. Yan and Q. W. Wang, *Catal. Commun.*, 2015, **66**, 67; c) F. Guo, W. L. Shi, X. Yan, Y. Guo and G. B. Che, *Sep. Puri. Tech.*, 2015, **141**, 246.
- 26 a) Z. J. Sun, Q. D. Yue, J. S. Li, J. Xu, H. F. Zheng and P. W. Du, *J. Mater. Chem. A*, 2015, **3**, 10243; b) S. S. Yi, X. Z. Yue, D. D. Xu, Z. P. Liu, F. Zhao, D. J. Wang and Y. H. Lin, *New J. Chem.*, 2015, **39**, 2917.
- 27 H. T. Ren, S. Y. Jia, Y. Wu, S. H. Wu, T. H. Zhang and X. Han, *Ind. Eng. Chem. Res.*, 2014, **53**, 17645.